



Supplementary Materials for

Gliogenic LTP spreads widely in nociceptive pathways

M. T. Kronschläger, R. Drdla-Schutting, M. Gassner,
S. D. Honsek, H. L. Teuchmann, J. Sandkühler*

*Corresponding author. Email: juergen.sandkuehler@meduniwien.ac.at

Published 10 November 2016 on *Science* First Release
DOI: 10.1126/science.aah5715

This PDF file includes:

Materials and Methods
Figs. S1 to S6
References

Other Supplementary Material for this manuscript includes the following:
(available at www.sciencemag.org/cgi/content/full/science.aah5715/DC1)

Movie S1

Materials and Methods

All experiments were performed in accordance with the European Community's Council directives 2010/63/EU and the rules of the Good Scientific Practice Guide of the Medical University of Vienna. They were approved by the Austrian Federal Ministry for Education, Science and Culture. Animals were fed with a standard diet with access to food and water *ad libitum*.

Spinal cord slice preparation

Under deep isoflurane anesthesia, the lumbar spinal cord was removed from male Sprague-Dawley rats (aged 20 to 25 days) as described previously (31). Transverse spinal cord slices (L4 - L6, 500 - 600 μm thick) each with an attached dorsal root (length: 10 - 15 mm) were cut on a microslicer. For the recordings shown in Fig.1, 2 and S4A the dorsal roots of one slice were separated into halves for stimulation of two independent primary afferent inputs. The slices were incubated for 30 min at 32°C and then stored at room temperature ($\sim 21^\circ\text{C}$) in oxygenated incubation solution containing (in mM): 95 NaCl, 1.8 KCl, 1.2 KH_2PO_4 , 0.5 CaCl_2 , 7 MgSO_4 , 26 NaHCO_3 , 15 glucose, 50 sucrose, pH was 7.4, measured osmolarity 310 – 320 $\text{mosmol}\cdot\text{l}^{-1}$.

Electrophysiological recordings *in vitro*

A single slice was transferred to the recording chamber, where it was continuously superfused at a rate of 3 – 4 $\text{ml}\cdot\text{min}^{-1}$ with oxygenated recording solution. The recording solution was identical to the incubation solution except for (in mM): 127 NaCl, 2.4 CaCl_2 , 1.3 MgSO_4 , 0 sucrose.

All recordings were conducted at room temperature. Superficial dorsal horn neurons were visualized with Dodt infrared optics (32) using a 40x, 0.80 N.A. water immersion objective on an upright microscope. Lamina I was identified as the area located within a distance of less than 20 μm from the overlying white matter border. Only lamina I neurons were considered for the experiments and recorded in the whole-cell patch clamp configuration with glass pipettes (2 – 4 $\text{M}\Omega$) filled with internal solution (in mM): 120 potassium gluconate, 20 KCl, 2 MgCl_2 , 20 HEPES, 0.5 Na-GTP, 0.5 $\text{Na}_4\text{-EGTA}$, 2 $\text{Na}_2\text{-ATP}$, 7.5 Phosphocreatine disodium salt hydrate, pH 7.28 adjusted with KOH, measured osmolarity 310 $\text{mosmol}\cdot\text{l}^{-1}$. The patch pipettes were pulled on a horizontal micropipette puller from borosilicate glass. Voltage-clamp recordings were made at a holding potential of -70 mV using a patch clamp amplifier and an acquisition software package. Signals were low-pass filtered at 2 – 10 kHz, sampled at 20 kHz and analyzed offline.

Passive membrane properties

The resting membrane potential was measured immediately after establishing the whole-cell configuration. Only neurons with a resting membrane potential more negative than -50 mV were used for further analysis. Membrane resistance, membrane capacitance and series resistance were calculated from the averaged reaction to 20 consecutive hyperpolarizing voltage steps from -70 to -80 mV for 100 ms. Neurons with a calculated series resistance of more than 30 $\text{M}\Omega$ were excluded from further analysis.

Evoked Excitatory Postsynaptic Currents (EPSCs)

EPSCs were evoked by stimulating dorsal root afferents using a suction electrode with an isolated current stimulator. After determining the threshold value to elicit an EPSC, two consecutive pulses (0.1 ms pulse width, 300 ms time interval) were given at 15 s intervals. In slices where the dorsal roots were divided into halves, test stimuli were applied at 15 s intervals alternatively to one half. The intensity for test stimuli was set to 200% of the threshold value. Afferent input was classified as being C-fiber-evoked based on a combination of response threshold of > 1 mA and conduction velocity of < 1 m·s⁻¹ (33). C-fiber-evoked EPSCs were considered monosynaptic by the absence of failures during 10 consecutive pulses at 2 Hz and a jitter in response latencies lower than 10%. Only neurons fulfilling all these criteria were further analyzed. Series resistance was monitored throughout the recording by applying a square pulse of -10 mV for 10 ms at 15 s intervals. Neurons were discarded when the series resistance changed by more than 20% during the experiment. For every cell measured, we performed a paired t-test to evaluate whether EPSC amplitude at the end of the recording was significantly different from baseline. In addition, a minimum increase in EPSC amplitude of 10% was required to be considered a responder.

For LTP induction, conditioning high-frequency stimulation (HFS, 3 x 100 Hz for 1 s at 10 s intervals) was applied at 5 mA to the dorsal root or to one dorsal root half (conditioned input). Holding currents were set to zero during conditioning stimulation.

NPE-IP₃ uncaging and calcium imaging in astrocytes

Experiments were performed at room temperature in normal oxygenated recording solution. For UV-light-triggered rise in intracellular calcium ion concentration, astrocytic

networks were filled via patch-pipettes (3 – 6 M Ω resistance) as described previously (34). In brief, patch-pipettes were filled with an intracellular solution consisting of the following (in mM): 120 potassium gluconate, 20 KCl, 2 MgCl₂, 20 Hepes, 0.5 Na-GTP, 2 Na₂-ATP, 7.5 Phosphocreatine disodium salt hydrate, 0.4 F5F (to monitor intracellular calcium increases), 2 NPE-caged IP₃ (to induce the release of calcium from intracellular stores) as well as 0.01% sulforhodamine B (SRB, to visualize the network extension). For control recordings, NPE-caged IP₃ was omitted from the intracellular solution. After establishing the whole-cell configuration, electrophysiological properties were determined with an amplifier coupled to a digitizer and the pClamp10 software package. After confirming that recorded cells exhibited electrophysiological characteristics of astrocytes (low input resistance, linear current-voltage relationship, membrane potential more negative than –70 mV), the astrocytic network was filled for at least 30 min. After successful withdrawal of the patch pipette, a lamina I neuron with the cell body within the area of the filled astrocytic network was patched. Neuronal recordings were performed and analyzed as described above.

Uncaging of NPE-caged IP₃ in the astrocytic network was induced by UV-flashes applied via an optical fiber (365 μ m diameter, N.A. 0.22) coupled to a computer-controlled Xenon-Flashlamp system (settings C3/300 V). UV-light was band-pass (270 – 400 nm) and long-pass filtered (295 nm). UV-pulse trains consisted of three stimulations at 10 s intervals, during which 5 UV-flashes were applied at 5 Hz (i.e. 1 s stimulation at 15 s, 26 s and 37 s).

Calcium-imaging was performed via multiphoton imaging on a microscope equipped with a 20x objective (N.A. 1.0) and a Chameleon-XR Ti-sapphire laser. SRB and F5F

were excited at 820 nm, and fluorescence emission was collected with non-descanned detectors (NDDs) at 565 – 605 nm and 500 – 550 nm, respectively. Images were collected at 2 Hz for 60 s. Data were collected from somata of F5F-filled astrocytes in a single optical plane, located at the same level as the recorded lamina I neuron. Data are expressed as changes in fluorescence intensity relative to baseline fluorescence ($\Delta F/F$).

Animal surgery for *in vivo* experiments

Experiments were performed on male Sprague-Dawley rats weighing between 150 and 250 g. Isoflurane (4 vol%) in two thirds N₂O and one third O₂ was initially administered via a respiratory mask to induce anesthesia. Animals were intubated using a 16 G cannula and then mechanically ventilated at a rate of 75 strokes·min⁻¹ using a tidal volume of 4 – 6 ml. Anesthesia was maintained by 1.5 vol% isoflurane. Body core temperature was kept at 37.5°C with a feedback controlled heating blanket. Deep surgical level of anesthesia was verified by stable mean arterial blood pressure during noxious stimulation. Surgical procedures were performed as described previously (35). Briefly, a jugular vein and a carotid artery were cannulated to allow intravenous (i.v.) infusions and arterial blood pressure monitoring, respectively. Muscle relaxation was achieved by 2 µg·kg⁻¹·h⁻¹ i.v. pancuronium bromide. Following cannulation, the left sciatic nerve was dissected free for bipolar electrical stimulation with a silver hook electrode. The lumbar segments L4 and L5 were exposed by laminectomy. The dura mater was carefully incised and retracted. Two metal clamps were used for fixation of the vertebral column in a stereotactic frame. An agarose pool was formed around the exposed spinal segments. The spinal cord was continuously superfused with 5 ml artificial cerebrospinal fluid consisting of (in mM): 135 NaCl, 1.7 KCl, 1.8 CaCl₂, 10 HEPES, 1 MgCl₂, pH 7.4 adjusted with KOH,

measured osmolarity $290 \text{ mosmol}\cdot\text{l}^{-1}$ by means of a roller pump in a closed circuit system, in which additional drugs could be dissolved as indicated. For transfer experiments, the total volume of the superfusate (i.e. 5 ml) was collected from a donor animal one hour after conditioning HFS (or after one hour of baseline recordings for control recordings) and transferred to a recipient animal by replacing the superfusate circulating during baseline recording. At the end of each electrophysiological experiment, animals were decapitated under deep anesthesia. The spinal cord was removed and cryo-fixed for detection of a rhodamine B spot at the recording site under a fluorescence microscope. Only those experiments where the recording site was located in laminae I or II were analyzed further.

Electrophysiological recordings *in vivo*

Electrophysiological recordings were performed as described previously (35). Briefly, C-fiber-evoked field potentials were recorded with glass electrodes (impedance 2 – 3 M Ω) from laminae I and II of the spinal cord dorsal horn in response to stimulation of sciatic nerve fibers at C-fiber strength. The pipette solution consisted of 135 mM NaCl, 1.7 mM KCl, 1.8 mM CaCl₂, 10 mM Hepes, 1 mM MgCl₂ and 0.2% rhodamine B. At the end of each electrophysiological experiment the recording site was labelled by pressure application (300 mbar for 1 min) with 0.2% rhodamine B via the electrode. Electrodes were driven by a microstepping motor. Recordings were made with an amplifier using a band width filter of 0.1 – 1000 Hz. Signals were monitored on a digital oscilloscope and digitized by an A/D converter. Test stimuli were delivered to the sciatic nerve and consisted of pulses of 0.5 ms duration at 25 V applied every 5 min using an electrical

stimulator. LTP was induced by electrical HFS (four trains of 100 Hz, 60 V, 0.5 ms pulses for 1 s at 10 s intervals).

Drugs and drug administration

For *in vitro* recordings, all substances were added to the recording solution or to the intracellular solution at known concentrations as indicated. Drugs used were sulforhodamine B (SRB; 0.01%), 2' (3')-O-(4-Benzoylbenzoyl) adenosine 5'-triphosphate triethylammonium salt (BzATP, 100 μM), A-438079 (10 μM), Na-fluoroacetate (10 μM), catalase (300 $\text{U}\cdot\text{ml}^{-1}$), D-amino acid oxidase (DAAO, 0.2 $\text{U}\cdot\text{ml}^{-1}$), D-2-amino-5-phosphonopentanoate (D-AP5, 50 μM), D-myo-inositol trisphosphate-P4-1-(2-Nitrophenyl)ethyl-ester (NPE-caged IP_3 , 2 mM, [cag-0-145]), Fluo-5F (400 μM), MK-801 maleate (1 mM), 8-Cyclopentyl-1, 3-dipropylxanthine (DPCPX, 1 μM) and D-serine (100 μM). Slices were pre-incubated in fluoroacetate for recordings shown in Fig. 1C, 2Ac, 2Bc and S1E, and in DAAO and catalase for recordings shown in 2Ae and 2Be for at least 1 h before use. All other drugs were applied to a closed system of 10 or 20 ml recording solution.

For *in vivo* recordings, pancuronium bromide was administered as an i.v. infusion (2 $\mu\text{g}\cdot\text{kg}^{-1}\cdot\text{h}^{-1}$). All other drugs were dissolved in distilled water and added directly to a closed system of 5 ml artificial cerebrospinal fluid superfusate to obtain the desired concentration as indicated: Na-fluoroacetate (10 μM), DAAO (1 $\text{U}\cdot\text{ml}^{-1}$), D-serine (10 μM or 100 μM), D-AP5 (100 μM), the interleukin 1 receptor antagonist IL1-Ra (80 $\text{pg}\cdot\text{ml}^{-1}$) and the soluble TNF receptor (sTNFR; 1 $\mu\text{g}\cdot\text{ml}^{-1}$).

Statistical Analysis

C-fiber-evoked EPSCs were analyzed offline using pClamp10 and SigmaPlot12. For quantification of synaptic strength the peak amplitude of the evoked EPSCs was measured. The mean amplitude of 6 evoked EPSCs prior to substance application or conditioning stimulation served as control and was compared to the mean amplitude of 6 EPSCs at different time points within the recording as indicated in the figure legends (e.g. 0 – 3 min, 2 – 5 min, 7 – 10 min, 12 – 15 min, 17 – 20 min, 27 – 30 min). Data were tested for normality (Shapiro-Wilk test) and for equal variance. Statistical significance was tested with a one-way repeated measures analysis of variance (RM ANOVA) with Bonferroni post-hoc correction or with a paired t-test. In case normality failed, a Wilcoxon signed-rank test was performed. The critical value for statistical significance was set at $P < 0.05$. Values are presented as mean \pm 1 standard error of mean (SEM).

C-fiber-evoked field potentials were analyzed offline using pClamp10 and SigmaPlot12. For quantification, the area under the curve of C-fiber-evoked field potentials was determined. The mean area under the curve of 5 consecutive stable field potentials prior to conditioning stimulation, or application of the superfusates from donor animals in case of transfer-experiments, served as baseline control. Responses were normalized to the baseline in every animal. Data were tested for normality using the Shapiro-Wilk test. Unless otherwise indicated, RM ANOVA was performed to compare the different experimental protocols and treatments. In all experimental groups, baseline was compared to different time points during the recording (40 – 60 min, 160 – 180 min and 220 – 240 min, and 280 – 300 min in Fig. S6, respectively). ANOVA was followed by Bonferroni post-hoc correction. Nonparametric one-way RM ANOVA on ranks was

performed in the case of non-normality. RM ANOVA on ranks was corrected by Dunnett's test. The critical value for statistical significance was set at $P < 0.05$. Values are expressed as mean \pm 1 SEM.

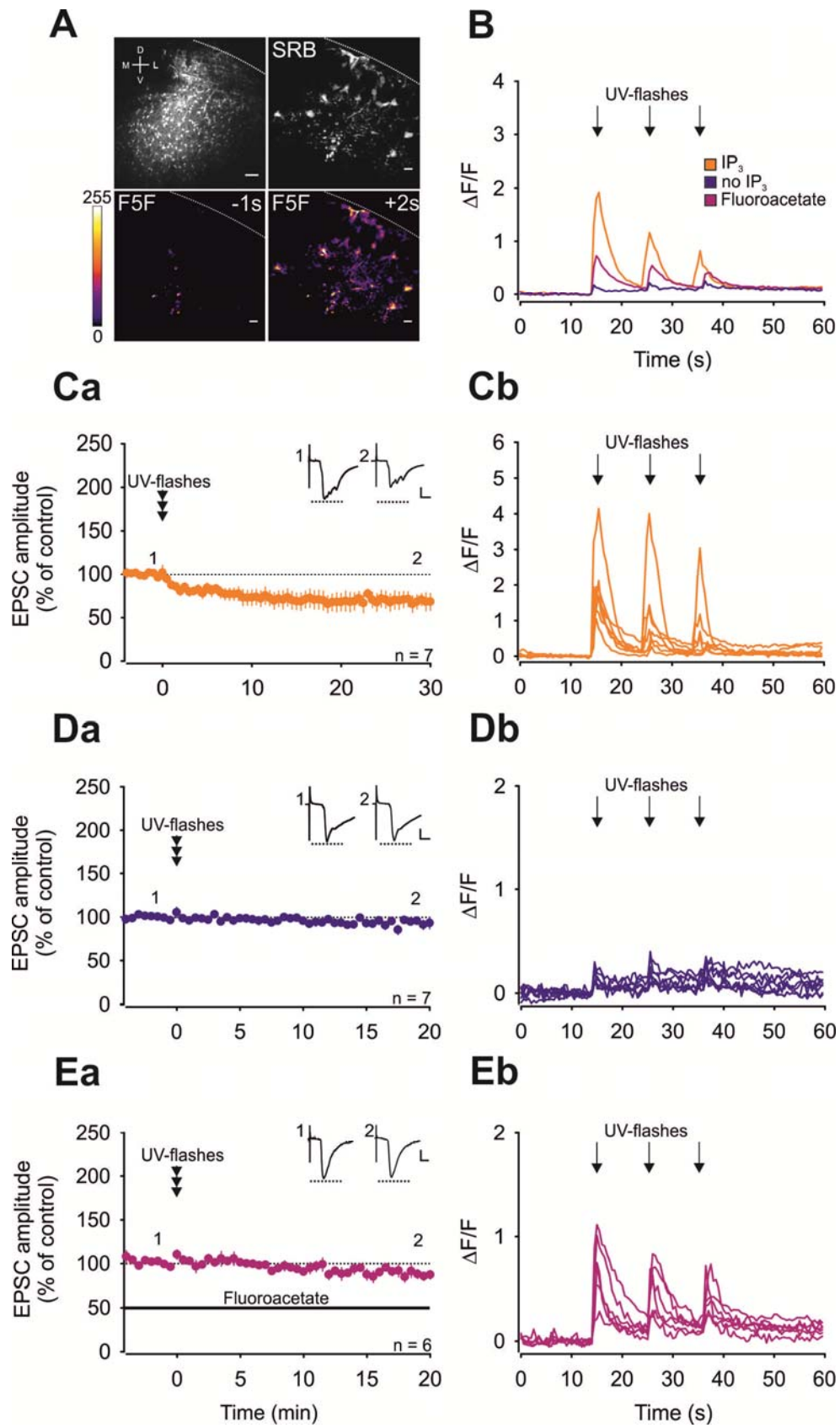


Fig. S1. Gliogenic LTD is induced at C-fiber synapses after IP₃ uncaging in astrocytic networks. (A) Dye coupling of astrocytes in the spinal dorsal horn. The white dotted lines mark the dorsal borders of the slices. Uncaging of IP₃ (2 mM) by application of UV-flashes (5 Hz, 3 x 1 s at 10 sec interval) induced an increase in [Ca²⁺]_i in astrocytes. The Fluo-5F (F5F) images are pseudo colored to indicate changes in F5F fluorescence intensity upon IP₃ uncaging. Calibration bars indicate 50 μm (top left) or 10 μm, respectively. (B) Mean change in F5F fluorescence intensity of astrocytes ($\Delta F/F$) in response to UV-flashes under three different conditions: IP₃ uncaging (orange trace; **Cb**), UV-flash application where IP₃ was omitted (purple trace; **Db**) and IP₃ uncaging under fluoroacetate (magenta trace; **Eb**). (Ca-Ea) EPSC recordings from lamina I neurons with monosynaptic C-fiber input lying within the areas of the astrocytic networks tested. Amplitudes of individual EPSCs were normalized to 6 baseline values and the mean (\pm 1 SEM) was plotted against time (min). (Ca) IP₃ uncaging in astrocytes induced LTD at C-fiber synapses (n = 7, P = 0.001, 30 min after UV-flashes compared to baseline). (Da) In the absence of caged IP₃, UV-flashes do not affect synaptic strength (n = 7, P = 0.061, 20 min after UV-flashes compared to baseline). (Ea) In the presence of fluoroacetate (10 μM), uncaging of IP₃ had no effect on synaptic transmission (n = 6, P = 0.112, 20 min after UV-flashes compared to baseline). During UV-flashes, holding currents were set to 0. Insets show individual EPSCs recorded at indicated time points. Calibration bars indicate 200 pA and 10 ms. Statistical significance was determined by using one-way repeated measures analysis of variance (RM ANOVA) followed by Bonferroni t-test. Paired t-test was used for control recordings.

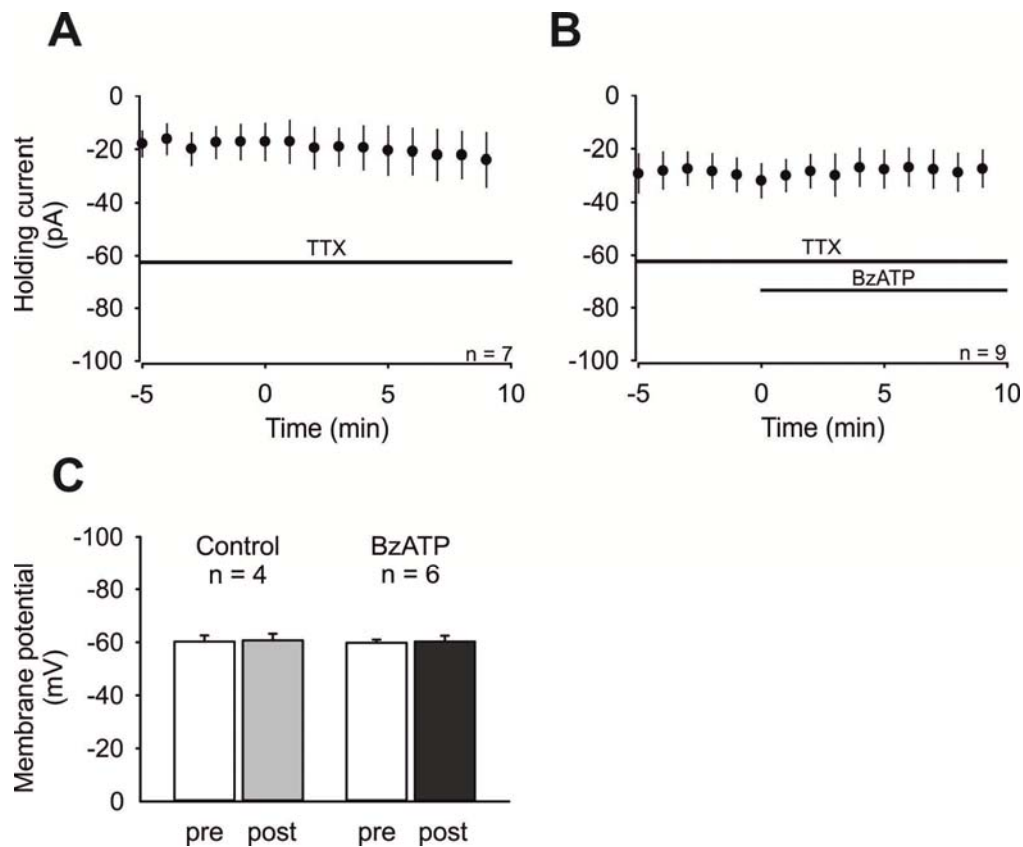


Fig. S2. Membrane properties of lamina I neurons are not changed by bath application of a P2X₇R agonist. Holding current and membrane potential recordings were performed on lamina I neurons. TTX (1 μ M) was bath-applied at least 3 min prior to recording. Data are expressed as mean \pm 1 SEM. Horizontal bars indicate drug application. **(A)** Holding current analysis of recorded neurons during TTX did not reveal any significant change over time (n = 7, $P = 0.345$ at 9 min compared to control values). **(B)** In the presence of TTX, BzATP (100 μ M) application starting at time point 0 min had no effect on holding currents (n = 9, $P = 0.556$ at 9 min compared to control values). **(C)** Membrane potential recordings in the presence of TTX were stable over time (grey

bar; $n = 4$, $P = 0.516$ at 10 min compared to baseline). BzATP (100 μM) was bath applied at time point 0 min and had no effect on the membrane potential (black bar; $n = 6$, $P = 0.851$ at 10 min compared to control values). In all experiments, statistical significance was determined by using a paired t-test.

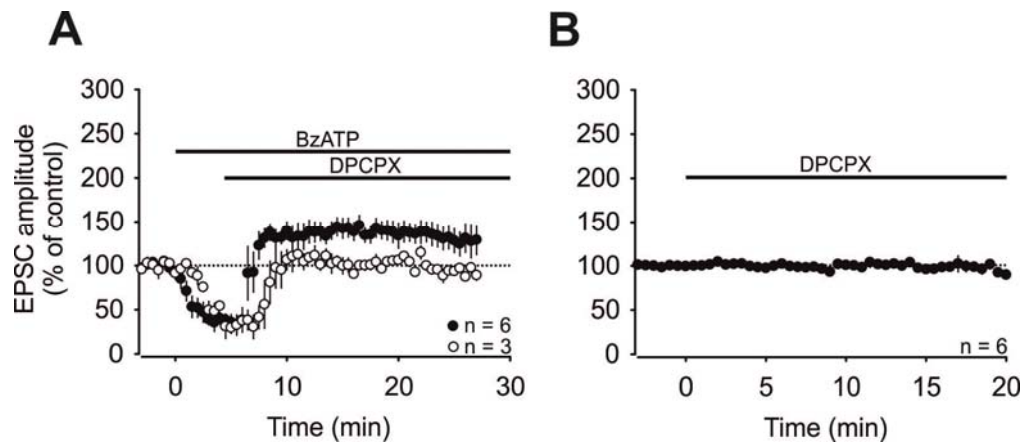


Fig. S3. Blockade of A₁ receptor signaling unmasks P2X₇R-mediated potentiation.

Recordings were performed on lamina I neurons with monosynaptic C-fiber input. Amplitudes of individual C-fiber-evoked EPSCs were normalized to 6 control values and the mean (\pm 1 SEM) was plotted against time (min). Horizontal bars indicate drug application. **(A)** Bath application of BzATP induced a significant depression of EPSC amplitudes at all C-fiber synapses tested (filled and open circles; $n = 9$, $P < 0.001$, 5 min after BzATP application compared to baseline). Blockade of A₁ receptors by DPCPX after BzATP application unveiled a P2X₇R-mediated potentiation of synaptic transmission in 6 out of 9 neurons (filled circles; $P = 0.003$, after 10 min of DPCPX application compared with control). In the remaining 3 neurons, blockade of A₁ receptor signaling reversed the BzATP-mediated depression to control values without inducing synaptic potentiation (open circles; $P = 1.0$, after 10 min of DPCPX application compared with control). **(B)** Blockade of A₁ receptor signaling with DPCPX alone had no significant effect on synaptic transmission at any of the C-fiber inputs tested ($n = 6$, $P = 0.853$, 20 min after DPCPX compared to baseline). Statistical significance was determined by using RM ANOVA followed by Bonferroni t-test. Paired t-test was used for control recordings.

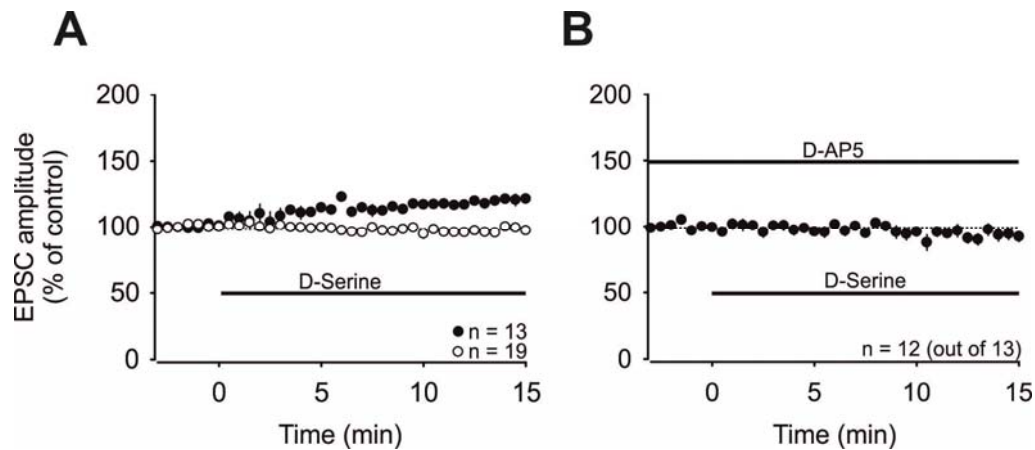


Fig. S4. D-Serine facilitates synaptic strength at spinal C-fiber synapses *in vitro*.

Recordings were performed on lamina I neurons with one (B) or two monosynaptic C-fiber inputs (A). Amplitudes of individual C-fiber-evoked EPSCs were normalized to 6 control values and the mean values (± 1 SEM) were plotted against time (min).

Horizontal bars indicate drug application. (A) D-Serine (100 μ M) added to the bath solution at time point 0 min induced amplification of synaptic strength at 13 out of 32 inputs tested (black circles; $P < 0.001$). In the remaining 19 inputs, D-serine failed to induce potentiation (open circles; $P = 0.04$). (B) In the presence of D-AP5 (50 μ M), bath application of D-serine had no effect on synaptic strength (n = 12 out of 13, $P = 0.094$, 15 min after D-serine compared to baseline). Statistical significance was determined by using paired t-test.

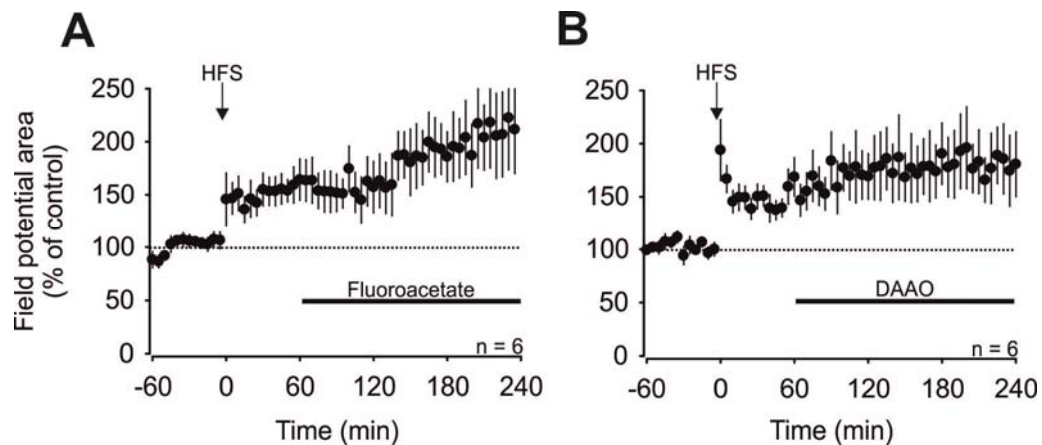


Fig. S5. Maintenance of HFS-induced LTP is not affected by inhibition of glial cell metabolism or by degradation of D-serine. Areas of C-fiber-evoked field potentials were normalized to baseline values and plotted against time (min). Data are expressed as mean \pm 1 SEM. LTP was induced by HFS at time point 0 min (arrow). Horizontal bars indicate drug application. **(A)** Spinal superfusion with the glial cell inhibitor fluoroacetate (10 μ M) had no effect on LTP maintenance throughout the recording period of 240 min ($n = 6$, $P = 0.433$). **(B)** Degradation of D-serine with DAAO (1 U \cdot ml $^{-1}$) did not affect maintenance of HFS-induced LTP ($n = 6$, $P = 0.546$). Statistical significance was determined by using RM ANOVA followed by Bonferroni t-test.

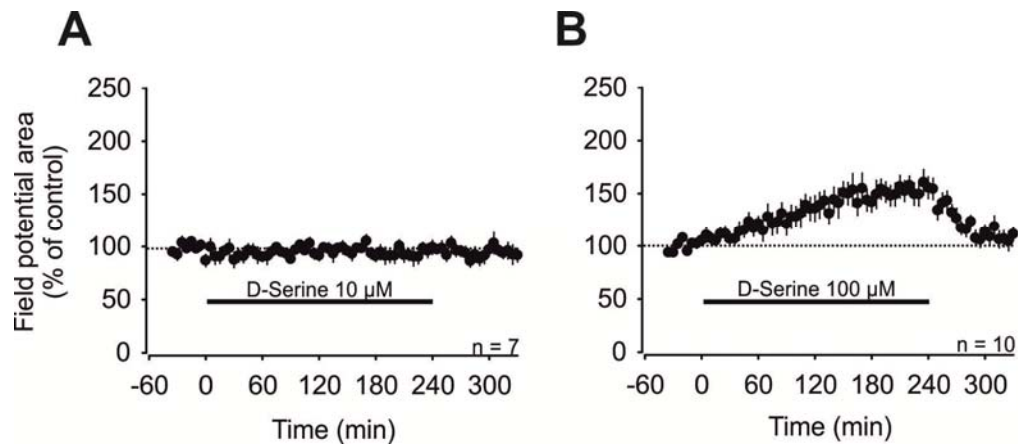


Fig. S6. D-Serine dose-dependently facilitates synaptic strength at spinal C-fiber synapses. Areas of C-fiber evoked field potentials were normalized to baseline values and plotted against time (min). Data are expressed as mean \pm 1 SEM. Horizontal bars indicate drug application. **(A)** D-Serine (10 μ M), which was added to the superfusate at time point 0 min for four hours had no effect on synaptic strength at C-fiber synapses (n = 7, $P = 0.510$). **(B)** A 10-fold higher concentration of D-serine (100 μ M) induced a steadily rising facilitation of synaptic strength ($P < 0.001$). Upon wash-out of D-serine, C-fiber mediated responses returned to baseline levels (n = 10, $P = 0.479$). Statistical significance was determined by using RM ANOVA on ranks followed by Dunnett's test.

Movie S1

NPE-IP₃ uncaging in spinal astrocytes upon UV-flash application.

References

1. T. V. P. Bliss, G. L. Collingridge, A synaptic model of memory: Long-term potentiation in the hippocampus. *Nature* **361**, 31–39 (1993). [Medline doi:10.1038/361031a0](#)
2. H. Ikeda, B. Heinke, R. Ruscheweyh, J. Sandkühler, Synaptic plasticity in spinal lamina I projection neurons that mediate hyperalgesia. *Science* **299**, 1237–1240 (2003). [Medline doi:10.1126/science.1080659](#)
3. H. Ikeda, J. Stark, H. Fischer, M. Wagner, R. Drdla, T. Jäger, J. Sandkühler, Synaptic amplifier of inflammatory pain in the spinal dorsal horn. *Science* **312**, 1659–1662 (2006). [Medline doi:10.1126/science.1127233](#)
4. R. Kuner, Central mechanisms of pathological pain. *Nat. Med.* **16**, 1258–1266 (2010). [Medline doi:10.1038/nm.2231](#)
5. X.-Y. Li, H. G. Ko, T. Chen, G. Descalzi, K. Koga, H. Wang, S. S. Kim, Y. Shang, C. Kwak, S. W. Park, J. Shim, K. Lee, G. L. Collingridge, B. K. Kaang, M. Zhuo, Alleviating neuropathic pain hypersensitivity by inhibiting PKMzeta in the anterior cingulate cortex. *Science* **330**, 1400–1404 (2010). [Medline doi:10.1126/science.1191792](#)
6. R. Drdla, M. Gassner, E. Gingl, J. Sandkühler, Induction of synaptic long-term potentiation after opioid withdrawal. *Science* **325**, 207–210 (2009). [Medline doi:10.1126/science.1171759](#)
7. R.-R. Ji, T. Berta, M. Nedergaard, Glia and pain: Is chronic pain a gliopathy? *Pain* **154** (Suppl 1), S10–S28 (2013). [Medline doi:10.1016/j.pain.2013.06.022](#)
8. S. B. McMahon, M. Malcangio, Current challenges in glia-pain biology. *Neuron* **64**, 46–54 (2009). [Medline doi:10.1016/j.neuron.2009.09.033](#)
9. P. M. Grace, M. R. Hutchinson, S. F. Maier, L. R. Watkins, Pathological pain and the neuroimmune interface. *Nat. Rev. Immunol.* **14**, 217–231 (2014). [Medline doi:10.1038/nri3621](#)
10. Q.-J. Gong, Y. Y. Li, W. J. Xin, Y. Zang, W. J. Ren, X. H. Wei, Y. Y. Li, T. Zhang, X. G. Liu, ATP induces long-term potentiation of C-fiber-evoked field potentials in spinal dorsal horn: The roles of P2X₄ receptors and p38 MAPK in microglia. *Glia* **57**, 583–591 (2009). [Medline doi:10.1002/glia.20786](#)
11. H. W. Tao, L. I. Zhang, F. Engert, M. Poo, Emergence of input specificity of LTP during development of retinotectal connections in vivo. *Neuron* **31**, 569–580 (2001). [Medline doi:10.1016/S0896-6273\(01\)00393-2](#)
12. A. K. Clark, D. Gruber-Schoffnegger, R. Drdla-Schutting, K. J. Gerhold, M. Malcangio, J. Sandkühler, Selective activation of microglia facilitates synaptic strength. *J. Neurosci.* **35**, 4552–4570 (2015). [Medline doi:10.1523/JNEUROSCI.2061-14.2015](#)
13. J. G. Gu, A. B. MacDermott, Activation of ATP P2X receptors elicits glutamate release from sensory neuron synapses. *Nature* **389**, 749–753 (1997). [Medline doi:10.1038/39639](#)
14. Y.-X. Chu, Y. Zhang, Y.-Q. Zhang, Z.-Q. Zhao, Involvement of microglial P2X7 receptors and downstream signaling pathways in long-term potentiation of spinal nociceptive

- responses. *Brain Behav. Immun.* **24**, 1176–1189 (2010). [Medline](#)
[doi:10.1016/j.bbi.2010.06.001](#)
15. K. Kobayashi, E. Takahashi, Y. Miyagawa, H. Yamanaka, K. Noguchi, Induction of the P2X7 receptor in spinal microglia in a neuropathic pain model. *Neurosci. Lett.* **504**, 57–61 (2011). [Medline](#) [doi:10.1016/j.neulet.2011.08.058](#)
16. R. Aoyama, Y. Okada, S. Yokota, Y. Yasui, K. Fukuda, Y. Shinozaki, H. Yoshida, M. Nakamura, K. Chiba, Y. Yasui, F. Kato, Y. Toyama, Spatiotemporal and anatomical analyses of P2X receptor-mediated neuronal and glial processing of sensory signals in the rat dorsal horn. *Pain* **152**, 2085–2097 (2011). [Medline](#) [doi:10.1016/j.pain.2011.05.014](#)
17. W.-J. He, J. Cui, L. Du, Y. D. Zhao, G. Burnstock, H. D. Zhou, H. Z. Ruan, Spinal P2X₇ receptor mediates microglia activation-induced neuropathic pain in the sciatic nerve injury rat model. *Behav. Brain Res.* **226**, 163–170 (2012). [Medline](#)
[doi:10.1016/j.bbr.2011.09.015](#)
18. C. Ficker, K. Rozmer, E. Kató, R. D. Andó, L. Schumann, U. Krügel, H. Franke, B. Sperlágh, T. Riedel, P. Illes, Astrocyte-neuron interaction in the substantia gelatinosa of the spinal cord dorsal horn via P2X7 receptor-mediated release of glutamate and reactive oxygen species. *Glia* **62**, 1671–1686 (2014). [Medline](#) [doi:10.1002/glia.22707](#)
19. J. Jung, Y. H. Shin, H. Konishi, S. J. Lee, H. Kiyama, Possible ATP release through lysosomal exocytosis from primary sensory neurons. *Biochem. Biophys. Res. Commun.* **430**, 488–493 (2013). [Medline](#) [doi:10.1016/j.bbrc.2012.12.009](#)
20. R. D. Fields, Y. Ni, Nonsynaptic communication through ATP release from volume-activated anion channels in axons. *Sci. Signal.* **3**, ra73 (2010). [Medline](#)
[doi:10.1126/scisignal.2001128](#)
21. D. Gruber-Schoffnegger, R. Drdla-Schutting, C. Hönigsperger, G. Wunderbaldinger, M. Gassner, J. Sandkühler, Induction of thermal hyperalgesia and synaptic long-term potentiation in the spinal cord lamina I by TNF- α and IL-1 β is mediated by glial cells. *J. Neurosci.* **33**, 6540–6551 (2013). [Medline](#) [doi:10.1523/JNEUROSCI.5087-12.2013](#)
22. K. J. Sekiguchi, P. Shekhtmeyster, K. Merten, A. Arena, D. Cook, E. Hoffman, A. Ngo, A. Nimmerjahn, Imaging large-scale cellular activity in spinal cord of freely behaving mice. *Nat. Commun.* **7**, 11450 (2016). [Medline](#) [doi:10.1038/ncomms11450](#)
23. M. Martineau, T. Shi, J. Puyal, A. M. Knolhoff, J. Dulong, B. Gasnier, J. Klingauf, J. V. Sweedler, R. Jahn, J. P. Mothet, Storage and uptake of D-serine into astrocytic synaptic-like vesicles specify gliotransmission. *J. Neurosci.* **33**, 3413–3423 (2013). [Medline](#)
[doi:10.1523/JNEUROSCI.3497-12.2013](#)
24. D. N. Xanthos, J. Sandkühler, Neurogenic neuroinflammation: Inflammatory CNS reactions in response to neuronal activity. *Nat. Rev. Neurosci.* **15**, 43–53 (2014). [Medline](#)
[doi:10.1038/nrn3617](#)
25. R.-R. Ji, Z. Z. Xu, G. Strichartz, C. N. Serhan, Emerging roles of resolvins in the resolution of inflammation and pain. *Trends Neurosci.* **34**, 599–609 (2011). [Medline](#)
[doi:10.1016/j.tins.2011.08.005](#)
26. X.-H. Wei, X. Wei, F. Y. Chen, Y. Zang, W. J. Xin, R. P. Pang, Y. Chen, J. Wang, Y. Y. Li, K. F. Shen, L. J. Zhou, X. G. Liu, The upregulation of translocator protein (18 kDa)

- promotes recovery from neuropathic pain in rats. *J. Neurosci.* **33**, 1540–1551 (2013). [Medline doi:10.1523/JNEUROSCI.0324-12.2013](#)
27. I. P. Chessell, J. P. Hatcher, C. Bountra, A. D. Michel, J. P. Hughes, P. Green, J. Egerton, M. Murfin, J. Richardson, W. L. Peck, C. B. Grahames, M. A. Casula, Y. Yiangou, R. Birch, P. Anand, G. N. Buell, Disruption of the P2X₇ purinoceptor gene abolishes chronic inflammatory and neuropathic pain. *Pain* **114**, 386–396 (2005). [Medline doi:10.1016/j.pain.2005.01.002](#)
 28. A. M. Basso, N. A. Bratcher, R. R. Harris, M. F. Jarvis, M. W. Decker, L. E. Rueter, Behavioral profile of P2X₇ receptor knockout mice in animal models of depression and anxiety: Relevance for neuropsychiatric disorders. *Behav. Brain Res.* **198**, 83–90 (2009). [Medline doi:10.1016/j.bbr.2008.10.018](#)
 29. B. S. Khakh, M. V. Sofroniew, Diversity of astrocyte functions and phenotypes in neural circuits. *Nat. Neurosci.* **18**, 942–952 (2015). [Medline doi:10.1038/nn.4043](#)
 30. A. Aguzzi, B. A. Barres, M. L. Bennett, Microglia: Scapegoat, saboteur, or something else? *Science* **339**, 156–161 (2013). [Medline doi:10.1126/science.1227901](#)
 31. B. Heinke, E. Gingl, J. Sandkühler, Multiple targets of μ -opioid receptor-mediated presynaptic inhibition at primary afferent A δ - and C-fibers. *J. Neurosci.* **31**, 1313–1322 (2011). [Medline doi:10.1523/JNEUROSCI.4060-10.2011](#)
 32. H. Dodt, M. Eder, A. Frick, W. Zieglgänsberger, Precisely localized LTD in the neocortex revealed by infrared-guided laser stimulation. *Science* **286**, 110–113 (1999). [Medline doi:10.1126/science.286.5437.110](#)
 33. R. Ruscheweyh, L. Forsthuber, D. Schoffnegger, J. Sandkühler, Modification of classical neurochemical markers in identified primary afferent neurons with A β -, A δ -, and C-fibers after chronic constriction injury in mice. *J. Comp. Neurol.* **502**, 325–336 (2007). [Medline doi:10.1002/cne.21311](#)
 34. S. D. Honsek, C. Walz, K. W. Kafitz, C. R. Rose, Astrocyte calcium signals at Schaffer collateral to CA1 pyramidal cell synapses correlate with the number of activated synapses but not with synaptic strength. *Hippocampus* **22**, 29–42 (2012). [Medline doi:10.1002/hipo.20843](#)
 35. R. Drdla-Schutting, J. Benrath, G. Wunderbaldinger, J. Sandkühler, Erasure of a spinal memory trace of pain by a brief, high-dose opioid administration. *Science* **335**, 235–238 (2012). [Medline doi:10.1126/science.1211726](#)